

LA-UR- 09-06786

Approved for public release;
distribution is unlimited.

| | |
|----------------------|---|
| <i>Title:</i> | Calculating Kinetics Parameters and Reactivity Changes with Continuous Energy Monte Carlo |
| <i>Author(s):</i> | Brian Kiedrowski, Forrest Brown, Paul Wilson |
| <i>Intended for:</i> | American Nuclear Society PHYSOR-2010, Pittsburgh, PA 9-14 May 2010 |



Los Alamos National Laboratory, an affirmative action/equal opportunity employer, is operated by the Los Alamos National Security, LLC for the National Nuclear Security Administration of the U.S. Department of Energy under contract DE-AC52-06NA25396. By acceptance of this article, the publisher recognizes that the U.S. Government retains a nonexclusive, royalty-free license to publish or reproduce the published form of this contribution, or to allow others to do so, for U.S. Government purposes. Los Alamos National Laboratory requests that the publisher identify this article as work performed under the auspices of the U.S. Department of Energy. Los Alamos National Laboratory strongly supports academic freedom and a researcher's right to publish; as an institution, however, the Laboratory does not endorse the viewpoint of a publication or guarantee its technical correctness.

CALCULATING KINETICS PARAMETERS AND REACTIVITY CHANGES WITH CONTINUOUS-ENERGY MONTE CARLO

Brian Kiedrowski* and Forrest Brown

Los Alamos National Laboratory
P.O. Box 1663 MS A143, Los Alamos, NM 87545
bckiedro@lanl.gov; fbrown@lanl.gov

Paul Wilson

Department of Engineering Physics
University of Wisconsin-Madison
1500 Engineering Drive, Madison, WI 53706
wilsonp@engr.wisc.edu

ABSTRACT

The iterated fission probability interpretation of the adjoint flux forms the basis for a method to perform adjoint weighting of tally scores in continuous-energy Monte Carlo k -eigenvalue calculations. Applying this approach, adjoint-weighted tallies are developed for two applications: calculating point reactor kinetics parameters and estimating changes in reactivity from perturbations. Calculations are performed in the widely-used production code, MCNP, and the results of both applications are compared with discrete ordinates calculations, experimental measurements, and other Monte Carlo calculations.

Key Words: Monte Carlo, Adjoint Flux, Kinetics Parameters, Perturbation Theory

1. INTRODUCTION

The Monte Carlo method is used successfully for many calculations in nuclear reactor analysis. These include calculating k -eigenvalue, local assembly powers, dose rates, and numerous others. The major strength of Monte Carlo is that no discretization of phase space is necessary and therefore calculations can be done with highly-detailed geometry and continuous-energy-angle physics[1].

One area of weakness is the difficulty computing reactor kinetics parameters or estimating reactivity changes from perturbations. Various techniques[2],[3] have been devised for estimating the delayed neutron fraction β or the neutron generation time Λ , but these approaches are either cumbersome, have difficulty getting statistically meaningful answers, or are approximate. Estimating the change in reactivity $\Delta\rho$ can be performed in continuous-energy Monte Carlo by using the differential operator technique[4], but this method has issues with eigenvalue problems: it fails to account for the change in the fission source. Note that there is a partial fix to this problem[5].

*B. Kiedrowski was a PhD student at Univ. of Wisc. working at LANL at the time of submission.

The difficulties stem from the issue of estimating the adjoint flux in continuous-energy Monte Carlo. The kinetics parameters and reactivity changes are ratios of integrals of adjoint-weighted quantities[6],[7] and a continuous-energy approach to calculating them requires all tally scores be weighted by their corresponding adjoint flux. There have been sophisticated techniques[8] proposed to calculate adjoint fluxes with continuous-energy Monte Carlo that involve inverting the random walk, but these have not been widely implemented because of their complexity.

For a critical reactor, the adjoint flux has a special correspondence with the forward particle behavior after a long time. If a neutron is introduced into such a reactor, it will go on to make progeny via a fission chain reaction and eventually a steady state distribution will be established corresponding to the fundamental mode of the system*. It can be shown with the appropriate initial and final conditions[7],[9] that the amplitude of this fundamental mode is directly proportional to the adjoint flux at the point where the neutron was introduced. This is often referred to as the iterated fission probability[10] interpretation of the adjoint flux[†].

The asymptotic population of progeny can be measured in a forward continuous-energy Monte Carlo simulation without much difficulty; there is no need for random walk inversion. Furthermore, this can be adapted to the standard power iteration method for solving the k -eigenvalue problem such that no new random walks or particle simulations are necessary. For the cost of extra storage of information and minimal increase in CPU time, it is possible to calculate all the adjoint-weighted tallies for computing both the reactor kinetics parameters and reactivity changes from small perturbations. The method is demonstrated in the Monte Carlo N-Particle (MCNP) code[11].

2. COMPUTATIONAL METHOD

A method is developed to weight tally scores by their corresponding adjoint flux many fission generations (cycles or iterations) later. Tallies are scored in the zeroth generation, stored, and weighted by the future population in some special future n th generation.

It is first important to introduce some terminology. The neutrons in the zeroth generation or *original generation* are called *progenitors*. More formally, a progenitor is defined as the set of all random walk states in the original generation sharing a common past and terminating with a fission neutron producing event. A *branching event* is where the random walk splits into more than one unique path. At branching events, a new progenitor state needs to be created because the random walk states in both no longer share the exact same common past even though some states are shared. Examples include $n,2n$ reactions and splitting from variance reduction. Implicit captures that cause the emission of fission neutrons terminate the set of states defining a progenitor and count as a fission neutron producing event. The progenitor's tally scores are called *original contributions* and are stored until the future n th generation. Information about the current progenitor state is given to all progeny at each fission event.

The generations between the zeroth generation and the n th are called *latent generations*. During

*While one neutron is used in the development of this idea, in reality it is the average behavior that is important since the radiation transport equation neglects stochastic fluctuations.

[†]An alternative derivation can be done by showing correspondence of the iterated fission probability with the adjoint flux term in the equation for the change in reactivity derived from perturbation theory.

these, no additional scores are made, but the progenitor information is passed onto all subsequent progeny.

Once the n th generation (or the *asymptotic generation*) is reached, the original contributions are weighted by their importance estimate or *asymptotic population*. Following this weighting, the adjoint-weighted tally scores are added to the global accumulators. This series of n generations and the zeroth generation define a *progenitor set*. After the completion of the progenitor set, a new one begins such that an original generation follows the asymptotic generation.

2.1. General Formulation of Adjoint-Weighted Tallies

The general form for an adjoint-weighted tally T is given by

$$T = \frac{1}{N} \sum_p \pi_p \omega_p. \quad (1)$$

N is the total source weight of progenitors in the simulation. The sum of original contributions or generalized tally scores for progenitor p is ω_p . This may be a track-length flux estimator, fission source point, or anything else. π_p is the asymptotic population measured in the distant or asymptotic generation.

The asymptotic population is calculated with a track-length estimator in the asymptotic generation:

$$\pi_p = \sum_{\tau \in p} \nu \Sigma_f w \ell_\tau. \quad (2)$$

The summation is over all tracks τ that have progenitor index p . ν is the average number of neutrons produced per fission and Σ_f is the macroscopic fission cross section at the current energy E of the track. The length of the track is ℓ_τ and the current weight of the particle is w .

2.2. Reactor Kinetics Tallies

Starting with the sourceless time-dependent radiation transport equation, it is possible to derive the point reactor kinetics equations[6]:

$$\frac{dn}{dt} = \frac{\rho - \beta}{\Lambda} n(t) + \sum_{i=1}^6 \lambda_i c_i(t), \quad (3)$$

$$\frac{dc_i}{dt} = \beta_i n(t) - \lambda_i c_i(t) \quad i = 1, \dots, 6. \quad (4)$$

These equations describe the time behavior of the neutron population n and the delayed neutron precursor populations c_i . The point reactor kinetics equations are valid under the assumption of space-time separability. Here ρ is the reactivity (commonly $(k - 1)/k$ where k is the fundamental eigenvalue or multiplication factor of the system), β is the effective delayed neutron fraction, Λ is the neutron generation time, β_i is the effective fraction of precursors of type i , and λ_i is the corresponding decay constant. From the derivation, it is possible to derive a formulation for the kinetics parameters β and Λ :

$$\beta = \frac{\langle \psi^\dagger \mathbf{B} \psi \rangle}{\langle \psi^\dagger \mathbf{F} \psi \rangle}, \quad (5)$$

$$\Lambda = \frac{\langle \psi^\dagger \frac{1}{v} \psi \rangle}{\langle \psi^\dagger \mathbf{F} \psi \rangle}. \quad (6)$$

Here ψ is the neutron (angular) flux, ψ^\dagger is the adjoint flux, \mathbf{F} is the operator for the total fission source, \mathbf{B} is the operator for the delayed component of the fission source, and v is the neutron speed. $\langle \cdot \rangle$ denotes an integration over all space, energy, and direction. β is the ratio of the adjoint-weighted delayed fission source to the adjoint-weighted total fission source. Λ is the ratio of the adjoint-weighted neutron density to the adjoint-weighted total fission source.

Some criticality experiments measure a related quantity called Rossi- α :

$$\alpha = -\frac{\beta}{\Lambda} = -\frac{\langle \psi^\dagger \mathbf{B} \psi \rangle}{\langle \psi^\dagger \frac{1}{v} \psi \rangle}. \quad (7)$$

The three integrals common to these quantities are the adjoint-weighted neutron density, total fission source, and delayed fission source. Each of these integrals will become and tally that can be obtained from the general formulation in (1) by substituting the appropriate forms of ω_p .

The adjoint-weighted neutron density has the original contribution of the flux track-length estimator multiplied by a factor of $1/v$. The tally takes the following form:

$$\left\langle \psi^\dagger \frac{1}{v} \psi \right\rangle = \frac{1}{N} \frac{1}{V} \sum_p \pi_p \sum_{\tau \in p} \frac{1}{v} w_0 \ell_\tau. \quad (8)$$

Here the tracks τ are in the original generation and each set of tracks with the same progenitor index are weighted by the same asymptotic population π_p . V is the volume of the reactor. Since the tallies are divided to obtain the kinetics parameters, the volume cancels and does not need to be calculated. w_0 is the source weight of the fission neutron and is used rather than the current particle weight. This arises because, in addition to the original contribution, the neutron production in the next generation is multiplied by the particle weight. The importance (or adjoint flux) is the asymptotic population from a hypothetical neutron introduced at this point, and to

avoid double counting the effect of particle weight, a factor of w_0/w must be applied. This leaves behind only the source weight as the multiplier.

The adjoint-weighted total fission source is simpler. Every cycle in the power iteration method, neutrons are sampled from fission source sites created in the previous generation or cycle. To tally the fission source (not adjoint weighted) in a desired region, sum up the source weight of each particle within the region. Adjoint weighting is done by remembering each source point and later weighting the source weight by its corresponding asymptotic population. Since the region of interest is the entire reactor,

$$\left\langle \psi^\dagger \frac{1}{k} \mathbf{F} \psi \right\rangle = \frac{1}{N} \frac{1}{V} \sum_p \pi_p w_{0,p}. \quad (9)$$

The delayed fission source follows similarly,

$$\left\langle \psi^\dagger \frac{1}{k} \mathbf{B} \psi \right\rangle = \frac{1}{N} \frac{1}{V} \sum_p \pi_p w_{0,p} \delta_\beta. \quad (10)$$

δ_β is defined to be one if the neutron is from delayed emission and zero otherwise. It is possible to further decompose the delayed fission source into each of its individual precursor components to estimate each β_i .

The factor of $1/k$ is present because of the fission source normalization each cycle in the power iteration method. The integrals in the equations for kinetics parameters do not have this factor. Therefore, for systems not in a critical configuration, some estimate of k needs to be multiplied by the tally score. In MCNP, the most self-consistent estimate is to multiply each score by the geometric mean of the collision estimates of k within the progenitor set; however, this is not the only way to do this.

By taking the appropriate ratios, it is possible to find the kinetics parameters. Each tally, strictly speaking, has an arbitrary multiplicative constant; however, this constant is the same and therefore divides away.

An issue with any Monte Carlo tally is computing the uncertainties. Computing the uncertainty of each tally is fairly easy with the appropriate definition of a score x_i . The individual tally score contains all the individual subscores associated with all progenitor states from the same history in the original generation. Computing the uncertainty of the tally mean \bar{x} is done with the standard definition of variance from statistics:

$$\sigma_{\bar{x}}^2 = \frac{1}{N-1} \left[\frac{1}{N} \sum_{i=1}^N x_i^2 - \bar{x}^2 \right]. \quad (11)$$

Computing the uncertainty of a ratio is a little trickier, but can be done using standard techniques

of error propagation. The uncertainty of a ratio $z = x/y$ can be found from the formula:

$$\left(\frac{\sigma_z}{z}\right)^2 = \left(\frac{\sigma_x}{x}\right)^2 + \left(\frac{\sigma_y}{y}\right)^2 + \frac{\sigma_{xy}^2}{xy}. \quad (12)$$

σ_{xy}^2 is the covariance of random variables x and y . The covariance of two tallies with means \bar{x} and \bar{y} is

$$\sigma_{\bar{x}\bar{y}}^2 = \frac{1}{N-1} \left[\frac{1}{N} \sum_{i=1}^N x_i y_i - \bar{x}\bar{y} \right]. \quad (13)$$

The accumulators required to compute the kinetics parameters and their uncertainties are the sums of: the scores, the score squares, and the score products of each correlated tally.

2.3. Perturbation Tallies

By perturbing the radiation transport equation and assuming only first-order terms are significant[7], the change in reactivity from a perturbation can be approximated by

$$\Delta\rho = -\frac{\langle\psi^\dagger \mathbf{P}\psi\rangle}{\langle\psi^\dagger \mathbf{F}'\psi\rangle}. \quad (14)$$

\mathbf{P} is the perturbation operator taking the form,

$$\mathbf{P} = \Delta\Sigma_t - \Delta\mathbf{S} - \frac{1}{k}\Delta\mathbf{F}. \quad (15)$$

Σ_t is the macroscopic total cross section and \mathbf{S} is the scattering source. From left to right, the terms, when operating on the flux, denote the following: the change in the collision rate, the change in the scattering source, and the change in the normalized fission source.

The denominator is the adjoint-weighted perturbed fission source $\mathbf{F}'\psi = (\mathbf{F} + \Delta\mathbf{F})\psi$. Many formulations have the denominator as the unperturbed fission source $\mathbf{F}\psi$. This further approximation is obtained by neglecting another term during the derivation.

Note that for equation (14) to be valid, the forward and adjoint flux cannot be significantly altered by the perturbation.

There are three terms in the numerator and one in the denominator that need to have tallies. The first term in the numerator, the collision rate perturbation, is the simplest. The tally is a track-length estimator with a multiplier being the change in the total cross section,

$$\langle \psi^\dagger \Delta \Sigma_t \psi \rangle = \frac{1}{N} \frac{1}{V} \sum_p \pi_p \sum_{\tau \in p} \Delta \Sigma_t w_{0,p} \ell_\tau. \quad (16)$$

The other tallies require more thought. It is possible to bias a source by modifying the weight of emitted particles. Doing this, one source can be made to look like another. Often this is done as a variance reduction technique called source biasing; this works under the restriction that all relevant regions of phase space in the modified source are sampled in the unmodified one. Here, the biased (perturbed) source will be estimated from the change in the source. The change in each source is the expected change in source weight of the neutrons.

The change in the scattering source can be estimated using this logic. The scattering laws (the kinematics of the scattering event) are assumed to be unchanged. With this approximation, the change in the scattering source is estimated by

$$\langle \psi^\dagger \Delta \mathbf{S} \psi \rangle = \frac{1}{N} \frac{1}{V} \sum_p \pi_p \sum_{s \in p} w_{0,p} \frac{\Delta \Sigma_s}{\Sigma_s}. \quad (17)$$

The ratio within the inner summation is the change in the scattering cross section to the scattering cross section at incident energy E' . This, coupled with the expected frequency of scattering events in the simulated and unperturbed case, estimates the expected change in the frequency of neutrons arising from scattering in the perturbed case. The inner summation itself refers to all scattering events with progenitor index p . At each scattering event, the term in the inner summation is added to the original contribution accumulator.

Assuming the fission source spectrum χ is unperturbed, the change in the fission source is

$$\left\langle \psi^\dagger \frac{1}{k} \Delta \mathbf{F} \psi \right\rangle = \frac{1}{N} \frac{1}{V} \sum_p \pi_p w_{0,p} \frac{\Delta(\nu \Sigma_f)}{\nu \Sigma_f}. \quad (18)$$

The perturbed fission source is a fairly easy extension:

$$\left\langle \psi^\dagger \frac{1}{k} \mathbf{F}' \psi \right\rangle = \frac{1}{N} \frac{1}{V} \sum_p \pi_p w_{0,p} \frac{(\nu \Sigma_f)'}{\nu \Sigma_f}. \quad (19)$$

The values of $\nu \Sigma_f$ must be taken at the incident energy, not the emission energy. This requires either the original cross sections or the incident energy from the previous generation be known in the following generation.

Combining these and taking the appropriate ratio approximates the reactivity change resulting from a small perturbation. Computing the uncertainties is much like with the kinetics parameters. The three terms in the numerator should become one score bypassing the need to correlate the individual tallies. The uncertainty of the ratio is propagated as with the kinetics parameters.

3. VALIDATION OF REACTOR KINETICS PARAMETERS

The results of the point reactor kinetics parameters are validated against discrete ordinates calculations and experimental measurements. The discrete ordinates calculations are done with Partisn[12] and validate the neutron generation time Λ . Experimental measurements of Rossi- α are used as a reference for the Monte Carlo estimates. It is found that truncating the iterated fission probability at five generations for these calculations is sufficient, and that has been done for all of the results in this paper.

3.1. Discrete Ordinates Λ Comparisons

A few test problems involving 1-D bare and reflected slabs or spheres are used to validate Λ . A brief description of each problem is given in Table I.

The values are computed with MCNP and from Partisn by manually folding together its output forward and adjoint fluxes. The number of spatial zones and angular ordinates are very fine to mitigate truncation errors. The cross sections used in both MCNP and Partisn are equivalent. The results of the test problem comparisons are given in Table II.

The results compare quite well and are within statistical uncertainty bounds for various configurations, energy spectra, and criticality states. This shows that the methods being used in the Monte Carlo are the same as those computed directly with discrete ordinates. Specifically, test case 8, the highly reflected slab, is particularly revealing. Traditional, non-adjoint weighted, methods fail to estimate Λ correctly in highly reflected systems because they overestimate the

Table I. Test problem descriptions used in validating Λ . G denotes the number of energy groups.

| Problem | G | Description |
|---------|-----|---|
| 1 | 4 | Thermal slab, fuel/moderator mix |
| 2 | 4 | Reflected thermal slab, metal fuel w/ low-Z Reflector |
| 3 | 4 | Bare fast slab |
| 4 | 4 | Reflected fast slab |
| 5 | 8 | Bare intermediate spectrum slab |
| 6 | 4 | Bare fast sphere |
| 7 | 4 | Reflected fast sphere |
| 8 | 4 | Highly reflected slab |
| 9 | 4 | Subcritical bare fast slab ($k = 0.78$) |
| 10 | 4 | Supercritical bare fast slab ($k = 1.14$) |

Table II. Partisn/MCNP Λ comparisons for multigroup test problems.

| Problem | Λ (Partisn) | Λ (MCNP) |
|---------|---------------------|-------------------------------|
| 1 | 14.1323 μ s | 14.1025 \pm 0.0545 μ s |
| 2 | 135.2222 μ s | 135.0876 \pm 0.2081 μ s |
| 3 | 9.7910 ns | 9.7938 \pm 0.0128 ns |
| 4 | 43.4107 ns | 43.5719 \pm 0.0913 ns |
| 5 | 112.0086 ns | 112.5003 \pm 0.4341 ns |
| 6 | 1.7211 ns | 1.7185 \pm 0.0022 ns |
| 7 | 10.1895 ns | 10.1969 \pm 0.0158 ns |
| 8 | 6.1221 μ s | 6.1115 \pm 0.0073 μ s |
| 9 | 10.1715 ns | 10.1714 \pm 0.0138 ns |
| 10 | 9.6725 ns | 9.6752 \pm 0.0131 ns |

impact of neutrons deep in the reflector. The fact that these results match the adjoint-weighted results from Partisn demonstrates that the appropriate importance weighting is being used in the Monte Carlo tallies.

3.2. Experimental Rossi- α Comparisons

A few experimental measurements of Rossi- α have been made for OECD/NEA benchmarks[13]. Corresponding MCNP input files in the criticality validation suite[14] are used for the Monte

Table III. Rossi- α Monte Carlo comparisons with experimental measurements of selected OECD/NEA benchmarks. ENDF/B-VI.5 nuclear data is used.

| Problem | Measured α (ms^{-1}) | Calculated α (ms^{-1}) |
|-----------|--|--|
| Godiva | -1110 \pm 20 | -1136 \pm 12 |
| Jezebel | -640 \pm 10 | -643 \pm 13 |
| Flatop-23 | -267 \pm 5 | -296 \pm 5 |
| BIG TEN | -117 \pm 1 | -122 \pm 2.5 |
| STACY-29 | -0.122 \pm -0.004 | -0.128 \pm 0.002 |
| WINCO-5 | -1.1093 \pm -0.0003 | -1.152 \pm 0.037 |

Carlo calculations. The corresponding values of Rossi- α are estimated with Monte Carlo using the adjoint weighting techniques.

The results are compared with the experimental measurements, and are displayed in Table III. The comparisons come out fairly well with the exception of the Flattop measurement; the others are close, but sometimes outside the measurement uncertainties. While these discrepancies merit investigation, comparing computer calculations to experimental measurements is always tricky because the models do not necessarily reflect all the details of the system at the time of measurement.

4. VALIDATION OF REACTIVITY CHANGES

Changes in reactivity resulting from various perturbations are often estimated by running two separate Monte Carlo calculations and computing the change in k . This method is the most accurate, but it is often difficult to get good statistical convergence on Δk . This direct calculation is used to generate the reference results for comparison with the adjoint weighting techniques.

Several different perturbation types are investigated using three different systems. The first is the bare, high-enriched uranium sphere, Godiva, which has its density and enrichment perturbed. The second is a 2-D Pressurized Water Reactor (PWR) model[15] with boron-10 concentration changed in the water and xenon-135 added to the fuel. The third is a homogeneous, cylindrical reactor that investigates control rod worth calculations.

4.1. Bare Highly Enriched Uranium Sphere

The Godiva experiment is typically modeled as a simple, bare sphere of uranium metal. Two classic perturbations involve varying the density and the enrichment of the sphere.

The first perturbation looks at changing the density in a 0.1 cm edge layer of the Godiva sphere. The density is perturbed in increments of ten percent downward until the region becomes vacuum and upward until the region has double the nominal density. The continuous-energy Monte Carlo estimates of the first-order reactivity changes are compared with multigroup calculations[16] from Partisn.

The results are compared in Figure 1. The “exact” result is made by calculating $\Delta\rho$ directly from two separate Partisn calculations. The first-order Monte Carlo and discrete ordinates results show agreement within two standard deviations and follow the first-order results better than the exact ones, as should be expected.

The second perturbation varies the enrichment of the uranium metal globally. The nominal enrichment is about 93.7% and is varied $\pm 5\%$ [‡]. k' is calculated using the Monte Carlo perturbation techniques and compared to a reference perturbed case for which k' is computed directly via Monte Carlo. The results of the calculated estimates versus the reference values of k' are displayed in Figure 2 and show decent agreement over this range with small deviation for very high enrichment.

[‡]For simplicity, the perturbation amount is in atom percent rather than weight percent. Also, the uranium-234 concentration is kept fixed and only the uranium-235 and uranium-238 fractions are changed.

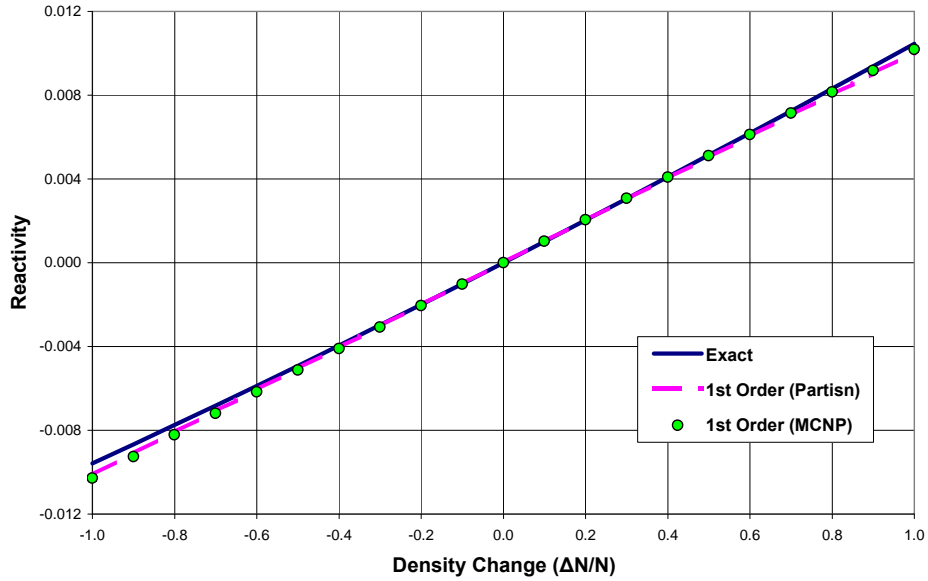


Figure 1. The density is varied in the outer 0.1 cm of the Godiva sphere. The discrete ordinates exact and first-order reactivity changes versus the Monte Carlo first-order estimates are compared. MENDF6 cross sections are used for the discrete ordinates and ENDF/B-VII.0 are used for the Monte Carlo. Error bars are displayed, but are too small to be seen.

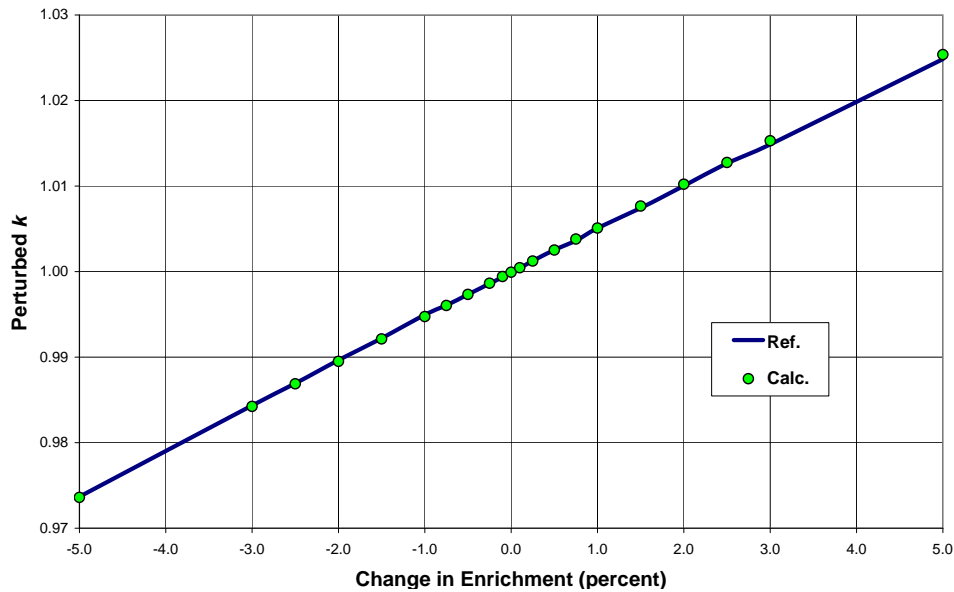


Figure 2. Enrichment variation in Godiva. First-order Monte Carlo estimates of the perturbed k versus those that are computed directly are displayed. ENDF/B-VII.0 data is used in the calculations. Error bars are displayed, but are too small to be seen.

4.2. Pressurized Water Reactor

A detailed 2-D PWR model is used to validate calculations of a realistic system. Two common aspects important to the operation of a PWR involve analyzing the impacts of the insertion of boron poison into the coolant (for reactivity control) and the natural buildup of the fission product xenon-135 in the fuel.

The critical concentration of boric acid in the coolant is found and perturbations are made by adding or removing the chemical shim. For simplicity, only the most relevant isotope, boron-10, is modeled and the water density is fixed. Like with the Godiva enrichment problem, a reference value of k' is computed directly from the perturbed case.

The comparison of the calculated and reference k' values are given in Figure 3. For modest changes in the boron-10 concentration, the results agree closely; however, for large changes in boron-10, the values differ significantly. This is because the central assumption that the forward and adjoint fluxes are not significantly perturbed is violated for large changes in boron concentration. A large perturbation will significantly change the absorption rate of thermal neutrons in the coolant, thereby altering the flux.

For the xenon buildup tests, the unperturbed case uses fresh fuel, and, for the perturbations, xenon-135 is added uniformly throughout the fuel at varying concentrations. In reality, the xenon-135 concentration will be a function of the local fission rate, however, simply adding the

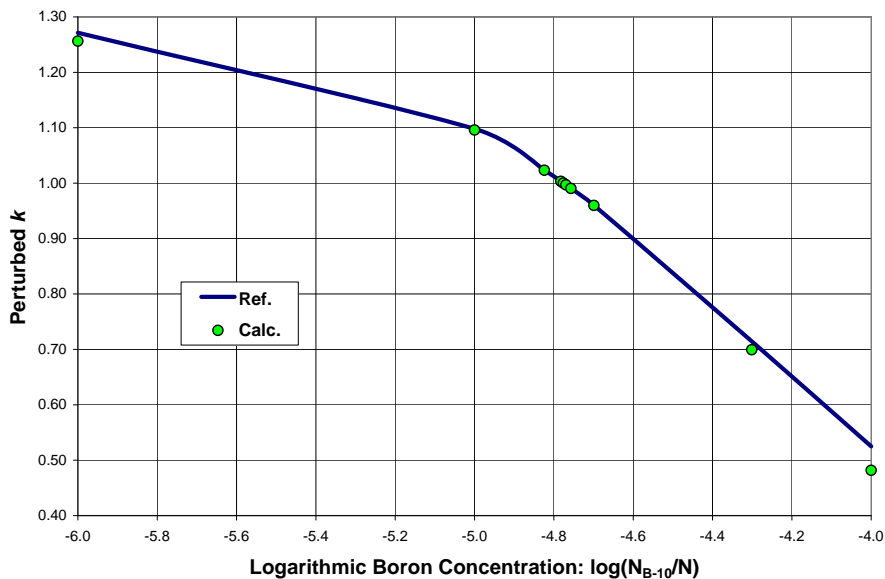


Figure 3. First-order Monte Carlo estimates of the perturbed k versus those that are computed directly. The boron-10 concentration is varied; the critical boron concentration is approximately 1.675×10^{-4} . ENDF/B-VII.0 data is used in the calculations. Error bars are displayed, but are too small to be seen.

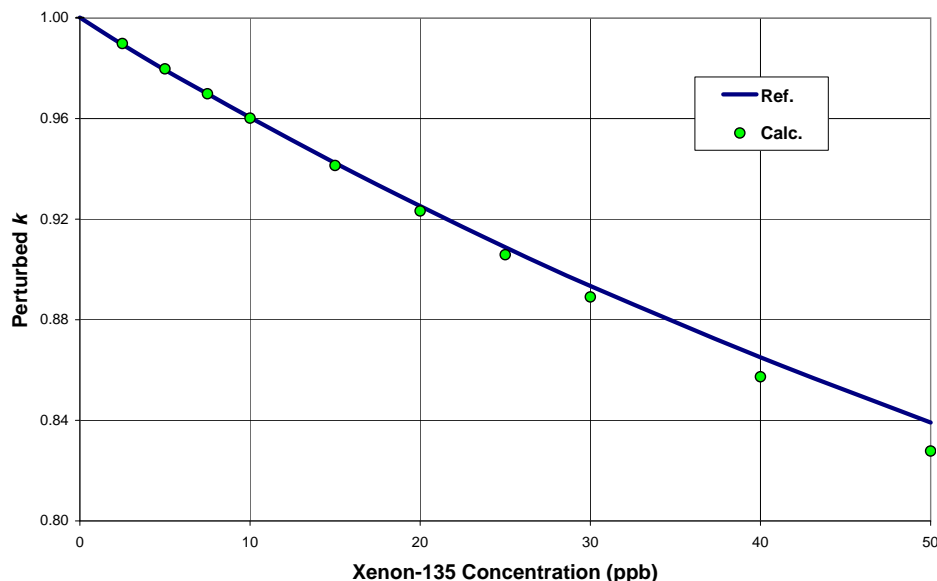


Figure 4. First-order Monte Carlo estimates of the perturbed k versus those that are computed directly. Xenon-135 is added uniformly to the fuel. ENDF/B-VII.0 data is used in the calculations. Error bars are displayed, but too small to be seen.

poison globally is adequate for proof-of-principle. Various concentrations of xenon-135 (in parts per billion or ppb) are added to the fuel and k' is estimated. The comparisons with reference Monte Carlo calculations are given in Figure 4. Like with the boron concentration calculations, good agreement is seen for small additions of xenon-135 to the fuel and less so for greater additions. The reasons for this are similar to those for large changes in boron concentration.

4.3. Control Rod Worth

A reflected, homogeneous cylindrical reactor is used to test whether this method can be used for control rod worth calculations. The cylinder has a height of 200 cm with an inner region with radius 100 cm and an outer region with radius of 150 cm. The inner region (atomic density of 9.02878×10^{-2} atoms per barn-cm) is a homogenous mixture of water, uranium oxide (UO_2 at 4% enrichment), and iron-56 in atomic fractions of 63.3%, 31.7%, and 5.0% respectively. The outer region is simply a water blanket surrounding the inner core region with atomic density of 2.3024×10^{-2} atoms per barn-cm.

The inner region is subdivided axially into three zones. The top zone contains a relative boron-10 concentration of 1.0×10^{-4} to simulate the addition of control rods from the top of the core. The bottom zone is the area where no control material has been inserted. The middle zone is 1 cm in length; it takes the property of the bottom zone in the unperturbed case, and has the material of the top zone in the perturbed case.

The differential rod worth, $d\rho/dz$, is approximated by the ratio of the change in reactivity $\Delta\rho$ to

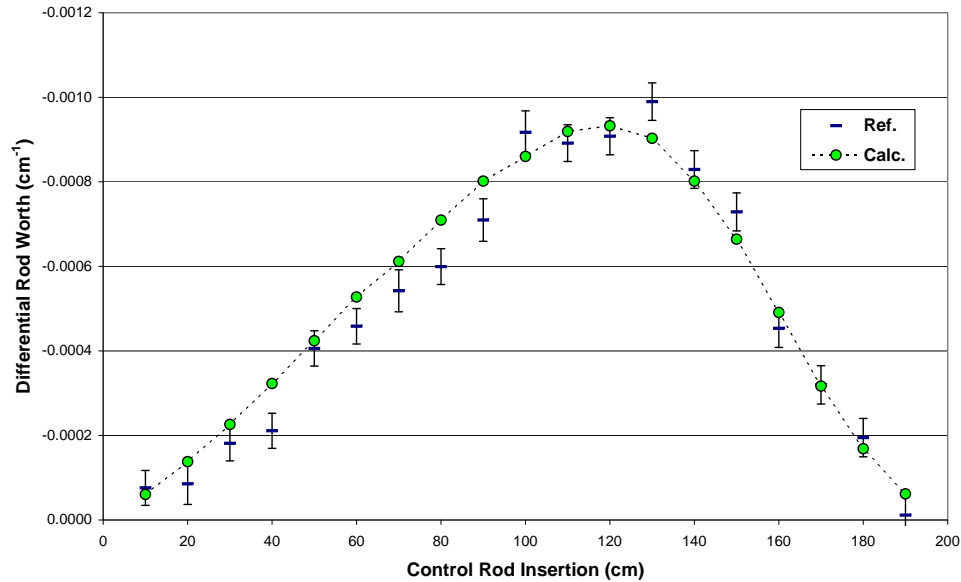


Figure 5. Differential control rod worth curves from the first-order perturbation method and the subtraction of two directly computed values of $1/k$. ENDF/B-VII.0 data is used in the calculations. Error bars are displayed for first-order estimates, but are too small to be seen.

the change in rod height Δz . The control rod bank height is given an unperturbed insertion starting from $z = 10$ cm and going in 10 cm increments to $z = 190$ cm. The perturbation is moving the entire control rod bank (represented by a homogeneous axial zone) downward by 1 cm. The differential rod worth estimates along with the reference values (obtained from subtracting $1/k$ obtained from two independent Monte Carlo calculations) are given in Figure 5. To help validate these results, figure 6 displays k estimated from an integral worth curve obtained from trapezoidal integration of the differential rod worth curve.

The first-order perturbation results produce a curve representative of what is expected; however, first-order perturbation theory may not be adequate for this calculation. As seen in Figure 6, the predicted values of k from the differential worths do not match the corresponding directly computed values. This is especially so when the control rods are deep into the core. In this regime, the flux becomes highly peaked at the bottom of the core. For even a small control rod insertion at this height, the resulting flux shift may be non-trivial. This invalidates the use of perturbation theory.

The values obtained from the adjoint weighting methods are much more stable statistically compared with the ones obtained from the subtraction of two stochastic numbers – the reference differential worths are computed with five times as many histories as the first-order estimates. While this conclusion cannot be generalized for every perturbation, it is possible to say that, for some classes of problems, significant improvements in efficiency can be made with this method over the old-fashioned approach of subtracting two values of $1/k$. This, of course, assumes that

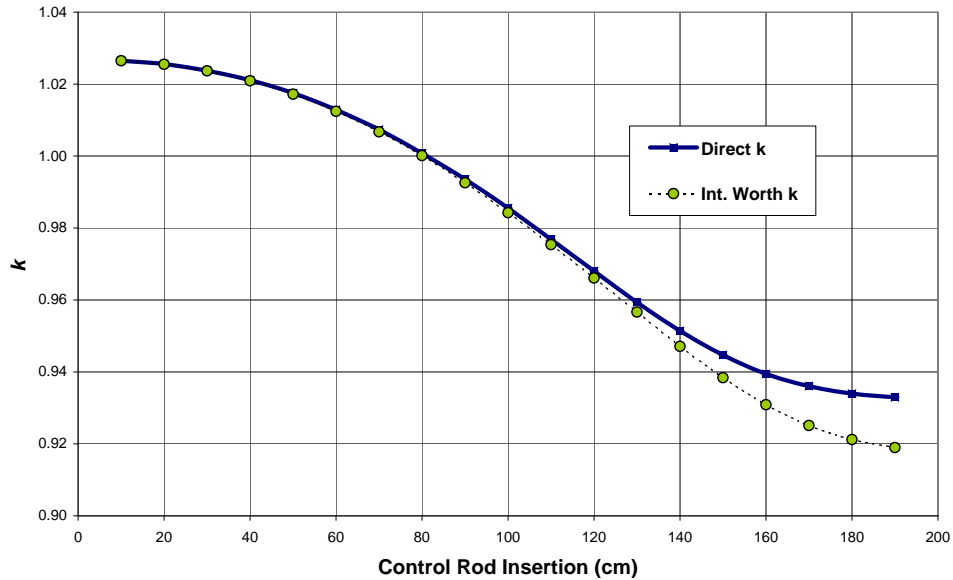


Figure 6. k values, for various rod insertions, estimated by the integral worth curve via trapezoidal integration of the differential worth curve in Figure 5. This is compared with k values computed directly at the given rod insertion. Error bars are displayed, but are too small to be seen.

first-order perturbation theory is valid for the calculation.

5. CONCLUSIONS & FUTURE WORK

The iterated fission probability interpretation of the adjoint flux enables the rigorous estimation of adjoint weighting factors in continuous-energy Monte Carlo k -eigenvalue calculations. Applied to specific tallies, this opens up the possibility of calculating properties of reactors that are defined as ratios of integrals of adjoint-weighted quantities. Specifically, the point reactor kinetics parameters and changes in reactivity via perturbation theory can be calculated effectively with this approach.

The adjoint-weighted tally methods can be further extended to other applications as well. For instance, very similar to perturbation theory is the notion of cross-section sensitivities. These sensitivities are particularly important for performing uncertainty analysis of nuclear data. Also, analyzing fixed-source multiplication of subcritical systems involves ratios of integrals of adjoint-weighted quantities as well.

Further analysis of the methods themselves still needs to be done. The largest question involves deciding how many generations are sufficient before measuring the asymptotic population. For global quantities, ad hoc rules of thumb are applied that work quite well; however, for local quantities or in systems with high dominance ratios, some form of convergence test may be required.

REFERENCES

- [1] F.B. Brown, "Monte Carlo Lectures," Los Alamos National Laboratory, LA-UR-05-4983 (2005).
- [2] R. Meulekamp and S.C. van der Marck, "Calculating Effective Delayed Neutron Fraction with Monte Carlo," *Nuclear Science and Engineering*, **152** pp. 142-148 (2006).
- [3] W.B. Verboomen, "Monte Carlo Calculation of Effective Neutron Generation Time," *Annals of Nuclear Energy*, **33** pp. 911-916 (2006).
- [4] H. Rief, "Generalized Monte Carlo Perturbation Algorithms for Correlated Sampling and a Second-Order Taylor Series Approach," *Annals of Nuclear Energy*, **11** pp. 455 (1984).
- [5] Y. Nagaya and F.B. Brown, "Estimation in the Change of k -effective due to Perturbed Fission Source Distribution in MCNP," *Proc. of M&C 2003, ANS Mathematics and Computation Meeting*, Gatlinburg, TN, Apr. 6-10 (2003).
- [6] G.R. Keepin, *Physics of Nuclear Kinetics*, Addison-Wesley, Reading, MA (1965).
- [7] G.I. Bell and S. Glasstone, *Nuclear Reactor Theory*, Van Norstrand Reinhold, New York, NY (1970).
- [8] J.E. Hoogenboom, "Methodology of Continuous-Energy Adjoint Monte Carlo for Neutron, Photon, and Coupled Neutron-Photon Transport," *Nuclear Science and Engineering*, **143** pp. 99-120 (2003).
- [9] J. Lewins, "The Time-Dependent Importance of Neutrons and Precursors," *Nuclear Science and Engineering*, **7** pp. 268-274 (1960).
- [10] A. Radkowsky (ed.), *Naval Reactor Physics Handbook*, vol. 1, pp. 864-849, Naval Reactors, U.S. Atomic Energy Commission (1964).
- [11] X-5 Monte Carlo Team, "MCNP - A General N-Particle Transport Code, Version 5, Volume I: Overview and Theory," Los Alamos National Laboratory, LA-UR-03-1987 (2003).
- [12] R.E. Alcouffe, R.S. Baker, et. al., "Partisn Manual," Los Alamos National Laboratory, LA-UR-02-5633 (2002).
- [13] J. Blair Briggs (ed.), *International Handbook of Evaluated Criticality Safety Benchmark Experiments*, Nuclear Energy Agency, NEA/NSC/DOC(95)03/I, Paris, France (2004).
- [14] R.D. Mosteller, "Validation Suites for MCNP," *Proc. 12th ANS Radiation Protection and Shielding Division Meeting*, Santa Fe, New Mexico, Apr. 14-17 (2002).
- [15] M. Nakagawa and T. Mori, "Whole Core Calculations of Power Reactors by use of Monte Carlo Method," *Journal of Nuclear Science and Technology*, **30**, no. 7, pp. 692-701 (1993).
- [16] J.A. Favorite, "Second-Order Reactivity Worth Estimates Using an Off-the-Shelf Multigroup Discrete Ordinates Transport Code," *Proc. of PHYSOR 2008, International Conference on the Physics of Reactors*, Interlaken, Switzerland, Sep. 14-19 (2008).